

Theoretical Study of the Bicyclic Nitrogen Tetroxide Cation, NO_4^+ Anatoli A. Korkin,[†] Marcel Nooijen,[†] Rodney J. Bartlett,^{*,†} and Karl O. Christe[‡]*Quantum Theory Project, University of Florida, Gainesville, Florida 32611-8435, and Phillips Laboratory, Edwards AFB, California 93524-7680 and Loker Research Institute, University of Southern California, Los Angeles, California 90089**Received: September 26, 1997; In Final Form: December 17, 1997*

The structure and energy of the bicyclic nitrogen tetroxide cation, D_{2d} NO_4^+ , and its C_{2v} transition state for dissociation into NO_2^+ and O_2 have been studied theoretically by the coupled-cluster (CC) and similarity-transformed equation-of-motion coupled-cluster methods (STEOM-CC). The computed 137 kcal/mol energy of decomposition and 370 kcal/mol gas-phase heat of formation identify NO_4^+ as a highly energetic species. Nevertheless, its low dissociation barrier (12–17 kcal/mol) and high vertical electron affinity (8.4 eV) indicate that NO_4^+ will have a low stability, which will complicate its experimental observation.

Introduction

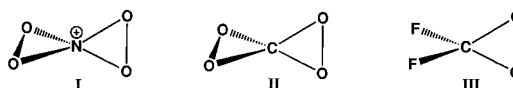
Nitrogen oxide cations, such as NO_2^+ and NO^+ , are strong oxidizers and useful components for ionic high energy density materials (HEDM).¹ The energy content and oxidizing power of these cations increase with the increasing oxidation state of the nitrogen atom and number of oxygen ligands. Our search for related, halogen-free, highly energetic cations has led to interest in the bicyclic NO_4^+ cation (**I**).

This novel cation contains twice as many oxygen ligands as NO_2^+ , and its energy content will be much higher due to the single-bond character of its N–O bonds. The energy barrier toward decomposition and electron affinity of NO_4^+ would be decisive for its possible experimental observation, methods of preparation, and application. Although the lattice interactions play a crucial role in stabilizing ions in solids, the synthesis and application of a species that is highly unstable toward unimolecular decomposition or has a large electronic affinity are questionable. It can be easily predicted that the stabilizing lattice interactions for NO_4^+ will be smaller than those for the existing ammonium cation, NH_4^+ , because of its larger size and the higher electronegativity of oxygen ligands compared with hydrogens, which leads to a shielding effect for the positive charge being localized on nitrogen in NO_4^+ .

In view of the great challenge presented by the synthesis of NO_4^+ and the potential for low-energy decomposition pathways, it was imperative to initially perform a feasibility study using ab initio methods. This contribution of theory offers the synthetic chemist the benefits of avoiding the unsuccessful pursuit of target molecules that are either vibrationally unstable or possess very low barriers toward decomposition.

No previous references to NO_4^+ (D_{2d}) could be found in the literature, and only the results of an ab initio quantum mechanical study of the isoelectronic carbon tetroxide, CO_4 (D_{2d}), have recently been published.² It was shown computationally that CO_4 (**II**) is a vibrationally stable, highly energetic molecule, 80 kcal/mol above the dissociation products, $\text{CO}_2 + \text{O}_2$ ($a^1\Delta_g$), with an estimated barrier of ~ 30 kcal/mol. Carbon tetroxide,

SCHEME 1



possessing two dioxirane rings, is also unknown experimentally. Furthermore, its close analogue, difluorodioxirane (**III**), has recently been synthesized and characterized,³ indicating that bis-dioxirane type compounds might also become synthetically accessible. (See Scheme 1 for structures of **I**, **II**, and **III**.)

It is possible that the actual symmetry of the transition state for decomposition is lower than C_{2v} , which will allow one bond to be broken initially; however, this may only reduce the barrier value, which appears to be very small even if we consider our estimate to be an upper limit. Possible tunneling effects and intersystem crossing interactions also can only reduce the barrier height. The same is true for decomposition pathways other than those considered here. It is also intuitively obvious that open-chain or branched forms of NO_4^+ will have biradical character, which in addition to the charge will ensure an extreme reactivity of these forms. Thus, we believe that no NO_4^+ isomers possess a reasonable stability and can only be observed as short-lived intermediates, if at all.

Computational Methods

The minimum energy structures and harmonic vibrational frequencies of D_{2d} NO_4^+ (**I**) (see Table 1) have been characterized at the HF, MBPT(2), and CCSD levels⁴ with double- ζ and triple- ζ basis sets (including polarization functions DZP and TZ2P, respectively)⁵ by using the ACES II program.⁶ Although single-determinant-based self-consistent field (SCF), perturbation, and coupled-cluster methods characterized successfully the minimum energy structure **I**, we failed to locate a transition state for decomposition by using the energy-following method.⁷ The reason for this failure was a multiconfigurational character to the wave function.

In searching for transition states and minima on the potential energy surface (PES) crossings, we use the recently developed similarity-transformed equation-of-motion method (STEOM)⁸ in its double-ionization version (i.e., DIP-STEOM). In general, the STEOM method proceeds by first performing a similarity

* Author to whom correspondence should be addressed.

[†] Quantum Theory Project.[‡] Phillips Laboratory.

TABLE 1: Bond Lengths (in angstroms) and Harmonic Vibrational Frequencies (in cm^{-1}) of D_{2d} NO_4^{+a}

parameter	method					
	HF/		MBPT(2)/		CCSD/	
	/DZP	/TZ2P	/DZP	/TZ2P	/DZP	/TZ2P
	bond lengths					
R_{NO}	1.290	1.292	1.346	1.347	1.335	1.335
R_{OO}	1.455	1.467	1.620	1.613	1.576	1.571
	frequencies					
B_1	472 (0)	466 (0)	341 (0)	340 (0)	376 (0)	377 (0)
E	556 (56)	553 (46)	511 (18)	499 (16)	505 (26)	499 (24)
A_1	696 (0)	689 (0)	563 (0)	571 (0)	554 (0)	567 (0)
B_2	942 (1)	942 (4)	664 (14)	692 (15)	679 (10)	716 (12)
E	1212 (24)	1173 (17)	967 (10)	949 (10)	1024 (16)	1005 (26)
A_1	1231 (0)	1218 (0)	913 (0)	929 (0)	981 (0)	998 (0)
B_2	1882 (100)	1832 (100)	1350 (100)	1355 (100)	1514 (100)	1502 (100)
	zero-point energies					
	12.52	12.29	9.70	9.70	10.24	10.25

^a Relative infrared intensities are given in parentheses.

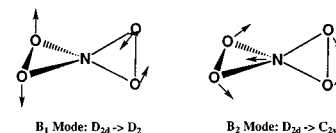
transformation of the Hamiltonian in second quantization, which accounts mainly for dynamical correlation. In the second step, this transformed Hamiltonian is diagonalized over a suitable and limited set of configurations, predominantly accounting for nondynamical correlation effects. In the present DIP case, the transformation is carried by performing a Hartree–Fock calculation on NO_4^- , which provides a reference determinant. Next, a CCSD calculation for the anion is performed that yields a first set of dynamical correlation amplitudes, T . Then, the so-called EOM-Hamiltonian, $\bar{H} = e^{-T}\text{He}^T$, is calculated and diagonalized over the 1-hole and 2-hole/1-particle configurations. This IP-EOM-CC calculation yields principal IPs of NO_4^- and therefore describes certain states of the NO_4 radical. It also provides a second set of amplitudes responsible for dynamical correlation effects that are used to define a doubly transformed Hamiltonian, $G = \{e^S\}^{-1}\bar{H}\{e^S\}$. Finally, this new Hamiltonian G (obtained in second quantization) is diagonalized over the 2-hole configurations, $\hat{\eta}|0\rangle$. The purpose of these transformations is to zero out matrix-elements in the Hamiltonian that couple to more highly excited determinants, such that the final diagonalization can be performed solely over a very small subspace. This procedure is equivalent to an implicit inclusion of dynamical correlation in the calculated energies.

The diagonalization over the 2-hole configurations yields the relevant set of states and energies of the NO_4^+ . These states are all properly symmetry and spin adapted, they contain a fair amount of dynamical correlation, and they have the proper multireference character. These attributes are reflected by the form of the final wave functions $\sum_{i,j} e^T \{e^S\} \hat{\eta}|0\rangle c_{ij}$.

The DIP–STEOM scheme is a very economical way to perform the calculations on this complicated system, the most expensive step being the CCSD calculation on the closed shell NO_4^- ground state. In our initial optimizations of the geometries, the CCSD amplitudes are replaced by their first-order perturbative analogue (which yields the MBPT(2) energy of the anion). In this STEOM–PT approximation, the most expensive step becomes the calculation of the EOM-Hamiltonian. All other steps in the correlated calculation take very little time, and the calculation of integrals is the dominant step in the calculation. This short time allows the use of numerical gradients to investigate the surfaces, including intersystem crossings, without a dramatic increase in computer time.

To locate a minimum at a crossing of two potential energy surfaces, we minimize the functional $F = E_1 + E_2 + \alpha *(E_1 - E_2)$, where α is a penalty parameter that typically has a value

SCHEME 2



of $\sim 10^3 - 10^4$. The DIP–STEOM calculation provides the energies E_1 and E_2 , allowing the use of numerical gradients on F in a straightforward manner.

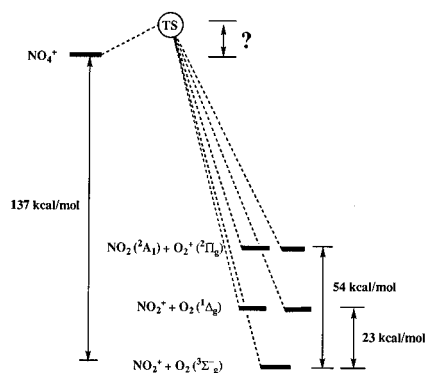
A drawback of the DIP–STEOM method is that orbitals optimized for the anion are used to describe the cationic states. Orbital relaxation effects can be fairly important for the cationic states and are difficult to describe in terms of mixing of configurations, but we assume that those are fairly similar for all cationic states and that our relative energetics are adequate. Also, the STEOM scheme assumes that dynamical correlation is rather small (otherwise the neglect of three-particle terms in the transformed Hamiltonian is not a valid approximation), meaning, primarily, that the CCSD calculation on NO_4^- needs to be a fair description of the anionic state over all geometries considered. However, at the D_{2d} geometry the lowest state of the anion is a triplet with two electrons in degenerate E-orbitals. In DIP–STEOM, the parent state must be a closed-shell and therefore the A_1 orbital is doubly occupied to create an anionic state. It is *not* necessary that the anion state actually exist, as it just provides a reference. The final estimates of the decomposition barrier have been obtained from STEOM-CCSD single-point calculations at the CCSD/DZP (D_{2d} minimum) and STEOM-CCSD/DZP (C_{2v} transition state) optimized geometries with an augmented basis set – PBS.⁹ We have also computed the CASPT2^{10,11} single-point energies with the ANO [*10s6p3d*] basis set¹² by using the MOLCAS program.¹³

Results and Discussion

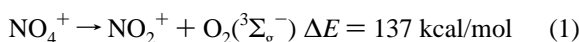
The nitrogen tetroxide cation is vibrationally stable at all levels of computation applied (see Table 1) and its lowest B_1 harmonic vibrational frequency, corresponding to a $D_{2d} \rightarrow D_2$ deformation, is 377 cm^{-1} at CCSD/TZ2P. The lowest B_2 vibrational frequency, corresponding to the $D_{2d} \rightarrow C_{2v}$ deformation in the direction of the minimum energy decomposition pathway is 716 cm^{-1} at that level (Scheme 2).

Although the harmonic vibrational frequencies of NO_4^+ do not include a very low B_2 frequency mode related to the C_{2v}

SCHEME 3



symmetry decomposition pathway, the high exothermicity of the decomposition of NO_4^+ shown in eq 1¹⁴ raises concerns about its experimental observation and the magnitude of its decomposition barrier:



The gas phase heat of formation of NO_4^+ (370 kcal/mol) has been estimated from eq 1 and the experimentally known heat of formation of NO_2^+ (233 kcal/mol).¹⁶ Although the heat of formation of ions in the solid state is considerably lower because of the lattice energy effect, the large endothermicity of its gas phase heat of formation indicates that NO_4^+ is a very energetic species.

The symmetry-forbidden C_{2v} minimum energy decomposition pathway links the ground-state NO_4^+ (1A_1) with the lowest singlet state of the decomposition products, NO_2^+ ($X^1\Sigma_g$) and O_2 ($^1\Delta_g$). The corresponding spin-forbidden decomposition pathway leads to the lowest triplet state, which is the combination of NO_2^+ ($X^1\Sigma_g^+$) and O_2 ($^3\Sigma_g^-$). The energy difference between the lowest singlet and triplet state of decomposition products is the singlet–triplet energy gap in O_2 , which is well-known experimentally to be 0.98 eV (22.6 kcal/mol).¹⁵ Because the energy difference between NO_4^+ and its decomposition products, NO_2^+ and O_2 , is large, the biradical combination of the dissociation products, $\text{NO}_2(^2A_1) + \text{O}_2(^2\Pi_g)$, which is ~54 kcal/mol above $\text{NO}_2^+(X^1\Sigma_g^+) + \text{O}_2(X^3\Sigma_g^-)$, but >80 kcal/mol below NO_4^+ ,¹⁶ should also be considered as being a possible important contributor in the multireference wave function of the decomposition transition state (Scheme 3).

Even a visual comparison of the occupied and unoccupied molecular orbitals of **I** and its decomposition products, NO_2^+ and O_2 (see Figure 1) shows that several MOs may change their character and occupation at the transition-state geometry, leading to a complicated pattern of the low-lying potential energy surfaces, including crossings and avoided crossings.

Our previous ab initio studies of the symmetry-forbidden minimum energy pathways for insertion of Be into H_2 (C_{2v} pathway)¹⁷ and for decomposition of N_4 (D_{2d} pathway)¹⁸ provide sufficiently accurate upper estimates of the corresponding reaction barrier energies, which are close to the energies of the lower symmetry transition states (N_4 ^{18,19}) and to the barriers found in multireference type computations (BeH_2 ¹⁷ and N_4 ²⁰). These encouraging results prompted us to use a similar approach in our search for the transition barrier energy and TS structure in the NO_4^+ decomposition.

To estimate stability of NO_4^+ , we used the DIP–STEOM method to search for the transition state and minima at the crossings of the NO_4^+ ground state (1A_1 in the C_{2v} symmetry group) and the lowest singlet (1B_1 , 1A_2 , 1B_2) and triplet (3A_1 ,

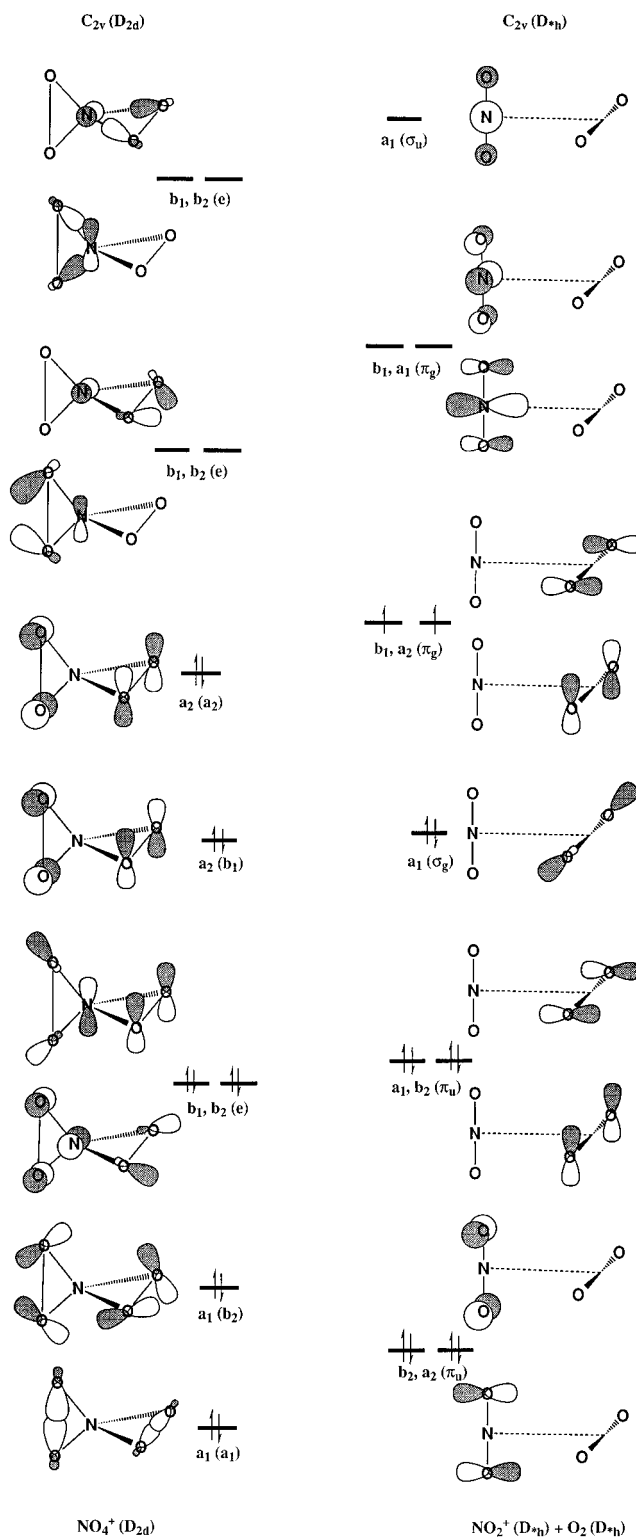


Figure 1. Highest occupied and lowest unoccupied molecular orbitals of NO_4^+ (1A_1) and separated NO_2^+ ($^1\Sigma_g^+$) and O_2 ($^3\Sigma_g^-$).

3B_1 , 3A_2 , 3B_2) excited-state potential energy surfaces. The transition state and two intersystem crossing minima have been located within a very narrow energy range of 11–13 kcal/mol above **I** at the STEOM-CCSD/PBS//STEOM-CCSD/DZP level (see Table 2).²¹ All other crossings occur at energies that are essentially lower than the transition barrier for decomposition, and their geometries show these structures to be “behind the

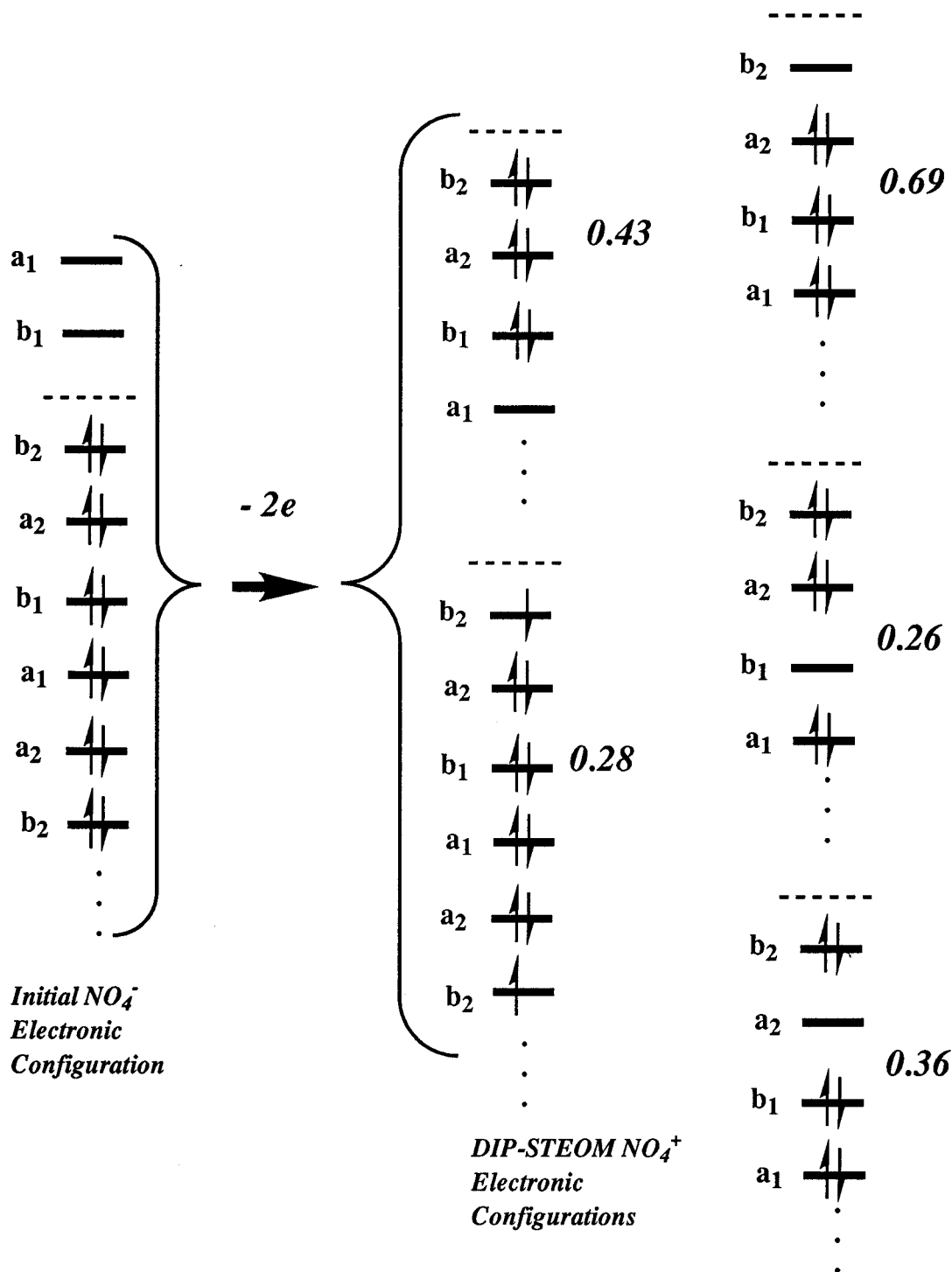


Figure 2. The character and the weights of the determinants in a multireference wave function for the NO_4^+ transition state generated by the DIP-STEOM method from the single reference NO_4^- wave function.

barrier" on the side of the decomposition products. These structures are not important for assessing the stability of NO_4^+ .

An intricate multiconfigurational character of the ground and excited states of NO_4^+ at the geometry of the transition state is demonstrated in Figure 2. The five different single-determinant configurations shown for the lowest 1A_1 state have large coefficients (>0.1). Two lowest singlet and triplet states of each symmetry have been computed at the transition state geometry (see Table 3). Three singlet (1B_1 , 1A_2 , and second 1A_1) and three triplet states (3B_1 , 3A_2 , and 3B_2) have energies within only a ± 5 kcal/mol range of that of the lowest 1A_1 state. All low-lying states except for the first triplet state of A_1

symmetry have a multiconfigurational character presented by CI coefficients in Table 3.

To verify our barrier energy estimate by another multiconfigurational approach, we have computed the single-point CASPT2/ANO energies for the minimum (CCSD/DZP) and the transition state (STEOM-CCSD/DZP). Eight orbitals (two of each symmetry) and 10 electrons have been included in the active space based on the character of the molecular orbitals and the corresponding (low)-energy single determinants of the minimum and transition state (see Figures 1 and 2). The 16.9 kcal/mol decomposition barrier energy computed at CASPT2 is in fair agreement with the 12 kcal/mol estimate obtained by

TABLE 2: Relative Energies (in kcal/mol)^a and Structures (Bond Lengths in Angstroms) of the Transition State and Minima at the PES Crossings for the C_{2v} Decomposition Pathway at the STEOM-CCSD/PBS//CCSD-STEOM/DZP Level^b

MO configuration	energy	R_{NO}^1	R_{NO}^2	R_{OO}^1	R_{OO}^2
minimum	0.0	1.335		1.576	
transition state	12.7	1.345	1.353	2.210	1.534
$^1A_1 - ^1B_1$ crossing	12.6	1.343	1.353	2.196	1.532
$^1A_1 - ^3B_1$ crossing	11.3	1.336	1.338	2.028	1.557

^a The total energy difference compared to the lowest D_{2d} structure (I). ^b The D_{2d} minimum has been computed at the CCSD/DZP level.

TABLE 3: Relative Energies (ΔE in kcal/mol) and the CI Coefficients of the Lowest Electronic States at the Transition State Geometry Computed at the STEOM-CCSD/PBS//CCSD/DZP Level

symmetry	ΔE	CI coefficients ^a			
3B_1	-5.0	0.85 (5b ₂ 2a ₂)	-0.43 (9a ₁ 4b ₁)	-0.26 (5b ₂ 1a ₂)	
1B_1	0.0	0.79 (5b ₂ 2a ₂)	-0.51 (9a ₁ 4b ₁)	-0.29 (5b ₂ 1a ₂)	
1A_1	0.4	0.71 (5b ₂ 5b ₂)	-0.44 (9a ₁ 9a ₁)	-0.34 (2a ₂ 2a ₂)	
		0.29 (4b ₂ 5b ₂)	0.23 (4b ₁ 4b ₁)		
1A_2	1.9	0.77 (5b ₂ 4b ₁)	-0.61 (9a ₁ 2a ₂)		
3A_2	2.3	0.80 (5a ₂ 4b ₁)	-0.58 (9a ₁ 2a ₂)		
1A_1	3.0	0.62 (2a ₂ 2a ₂)	-0.52 (4b ₁ 4b ₁)	0.42 (5b ₂ 5b ₂)	
		-0.27 (9a ₁ 9a ₁)	-0.23 (1a ₂ 2a ₂)	0.17 (4b ₂ 5b ₂)	
3B_2	4.1	0.97 (4b ₁ 2a ₂)	-0.24 (9a ₁ 5b ₂)		
3B_2	7.3	0.95 (9a ₁ 5b ₂)	0.22 (4b ₁ 2a ₂)	0.15 (9a ₁ 4b ₂)	
1B_1	31.2	0.93 (5b ₂ 1a ₂)	-0.33 (9a ₁ 4b ₁)		
3B_1	31.4	0.93 (5b ₂ 1a ₂)	-0.32 (9a ₁ 4b ₁)		
3A_1	43.9	1.0 (1a ₂ 2a ₂)			
1A_1	46.1	0.95 (1a ₂ 2a ₂)	-0.27 (4b ₁ 4b ₁)		

^a DIP-STEOM electronic configurations of NO_4^+ are presented as two electron holes in the single determinantal wave function of NO_4^- , which include nine a_1 , four b_1 , five b_2 , and two a_2 occupied MOs.

the STEOM method. Because we have imposed the C_{2v} symmetry of the decomposition path, our estimate of the barrier is an upper limit and the actual barrier value may be even lower because of the symmetry reduction and an avoided crossing of the molecular orbitals and the electronic states. We have not investigated lower than C_{2v} symmetry paths because of high computational costs.

Other characteristics important for the definition of stability and an experimental observation of a charged species are the electron affinity (electron attachment energy) of a cation and the (lowest) ionization potential (electron detachment energy) of an anion. Because NH_4^+ , which is the cationic component of ammonium nitrate NH_4NO_3 , is well characterized and may serve as a good reference species, we have computed the vertical electron affinities (EA_v) for NO_4^+ and NH_4^+ by the electron attachment method using the PBS basis set and the optimized coupled-cluster geometries (EOM-CCSD/PBS//CCSD/DZP).²² The EA_v of NO_4^+ (8.4 eV) was much higher than that of NH_4^+ (4.5 eV). The high electron affinity is an additional indication of the low feasibility for the existence of NO_4^+ , particularly taking into account that the lattice stabilization effect is expected to be smaller for NO_4^+ than for NH_4^+ . Nitrogen tetroxide has a larger size and the reverse electronegativity difference between the central nitrogen atom and ligands compared with ammonium cation. Although Mulliken charges are highly sensitive to the basis set, the trends and qualitative comparisons can be easily derived in this case. Thus oxygen atoms are almost neutral and provide a shielding effect for the positive charge toward external anions in NO_4^+ , whereas in NH_4^+ the positive charge is enhanced and delocalized at hydrogen atoms, which allow strong interactions with an anionic shell.

Conclusion

The bicyclic D_{2d} NO_4^+ cation is a highly energetic species with an estimated decomposition energy of 137 kcal/mol and gas-phase heat of formation of 370 kcal/mol. However, its low decomposition barrier (12–17 kcal/mol) and high vertical electron affinity (8.4 eV) will make its experimental observation difficult and would severely limit its potential usefulness.

It is possible that the actual symmetry of the transition state for decomposition is lower than C_{2v} , which will allow one bond to be broken initially; however, this situation may only further reduce the barrier value, which appears to be very small even if we consider our estimate to only be an upper bound. Possible tunneling effects and intersystem crossing interactions also can only reduce the barrier height. The same is true for decomposition pathways other than those considered here. It is also intuitively obvious that open-chain or branched forms of NO_4^+ will have biradical character that in addition to the charge, will ensure an extreme reactivity for such forms. Thus, we believe that no NO_4^+ isomer possesses a reasonable stability; therefore, these isomers can only be observed as short-lived intermediates, if at all.

Acknowledgment. This work is supported by the AFOSR under grant F49620-95-1-0130 (at the University of Florida) and by the National Science Foundation (at the University of Southern California). We thank Dr. M. Cory for his help with CASPT2 calculations.

References and Notes

- (1) Lawless, E. W.; Smith I. C. *Inorganic High-Energy Oxidizers*; Marcel Dekker: New York, 1968.
- (2) Averyanov, A. S.; Khait, Yu. G.; Puzanov, Yu. V. *J. Mol. Struct.* **1996**, *367*, 87.
- (3) (a) Russo, A.; Des Marteau, D. D. *Angew. Chem., Int. Ed. Engl.* **1993**, *32*, 905. (b) Kraka, E.; Konkoli, Z.; Cremer, D.; Fowler, J.; Schaefer, H. F. *J. Am. Chem. Soc.* **1996**, *118*, 10595.
- (4) Bartlett, R. J.; Stanton, J. F. In *Reviews in Computational Chemistry*; Lipkowitz, K. B., Boyd, D. B., Eds.; VCH: New York, 1994; Vol. 5, Chapter 2.
- (5) (a) Dunning, T. H. *J. Chem. Phys.* **1970**, *53*, 2823. (b) Dunning, T. H. *J. Chem. Phys.* **1971**, *55*, 716.
- (6) ACES II is a program product of the Quantum Theory Project, University of Florida. Stanton, J. F.; Gauss, J.; Watts, J. D.; Nooijen, M.; Oliphant, N.; Perera, S. A.; Szalay, P. G.; Lauderdale, W. J.; Gwaltney, S. R.; Beck, S.; Balkova, A.; Bernholdt, D. E.; Baeck, K.-K.; Rozyczko, P.; Sekino, H.; Huber, C.; Bartlett, R. J. Integral packages included are VMOL (Almlöf, J and Taylor, P. R.); VPROPS (Taylor, P. R.); ABACUS (Helgaker, T.; Aa Jensen, H. J.; Jørgensen, P.; Taylor, P. R.).
- (7) Banerjee, A.; Adams, N.; Simons, J.; Shepard, R. *J. Phys. Chem.* **1985**, *89*, 52.
- (8) (a) Nooijen, M.; Bartlett, R. J. *J. Chem. Phys.* **1997**, *106*, 6441; (b) *ibid.*, in press.
- (9) Sadlej, A. *Theor. Chim. Acta* **1991**, *79*, 123.
- (10) Andersson, K.; Malmqvist, P.-Å.; Roos, B. O.; Sadlej, A. J.; Wolinski, K. *J. Chem. Phys.* **1990**, *94*, 5483.
- (11) Andersson, K.; Roos, B. O. In *Modern Electronic Structure Theory, Part I*; Yarkony, D. R., Ed.; World Scientific: Singapore, 1995.
- (12) Widmark, P.-O.; Malmqvist, P.-Å.; Roos, B. O. *Theor. Chim. Acta* **1990**, *77*, 291.
- (13) *MOLCAS version 3*; Anderson, K.; Fulscher, M. P.; Karlström, G.; Lindh, R.; Malmqvist, P.-Å.; Olsen, J.; Roos, B. O.; Sadlej, A. J.; Blomberg, M. R. A.; Siegbahn, P. E. M.; Kellö, V.; Noga, J.; Urban, M.; Widmark, P.-O.
- (14) The total energies in eq 1 were computed at the CCSD(T)/TZ2P level with and without zero-point energy correction.
- (15) Huber, K. P.; Herzberg, G. *Constants of diatomic molecules*; Van Nostrand Reinhold: New York, 1979.
- (16) Lias, S. G.; Bartmess, J. E.; Liebman, J. F.; Holmes, J. L.; Levin, R. D.; Mallard, W. G. Gas-Phase Ion and Neutral Thermochemistry. *J. Phys. Chem. Ref. Data* **1988**, *Vol. 17*, Suppl. No. 1.
- (17) Purvis, III, G. D.; Shepard, R.; Brown, F. B.; Bartlett, R. J. *Int. J. Quantum Chem.* **1983**, *23*, 835.
- (18) Korin, A. A.; Balkova, A.; Bartlett, R. J.; Boyd, R. J.; Schleyer, P.v.R. *J. Phys. Chem.* **1996**, *100*, 5702.

(19) (a) Lauderdale, W. J.; Myers, W. J.; Bernholdt, D. E.; Stanton, J. F.; Bartlett, R. J. *Proceedings of the High Energy Density Materials Contractors Conference*, 25–28 February, Long Beach, CA, Phillips Lab. Edwards Air Force Base: 1990; p 121. (b) Lauderdale, W. J.; Stanton, J. F.; Bartlett, R. J. *J. Phys. Chem.* **1992**, *96*, 1174.

(20) Dunn, K. M.; Morokuma, K. *J. Chem. Phys.* **1995**, *102*, 4904.

(21) Because the lowest singlet state of the $D_{2d}NO_4^-$ is degenerate (see Figure 1), the minimum energy structure of NO_4^+ has been defined from optimization at the CCSD/DZP level.

(22) Nooijen, M.; Bartlett, R. J. *J. Chem. Phys.* **1995**, *102*, 3629.